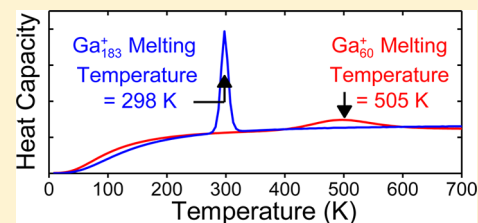


# Melting of Size-Selected Gallium Clusters with 60–183 Atoms

Katheryne L. Pyfer, Jared O. Kafader, Anirudh Yalamanchali, and Martin F. Jarrold\*

Chemistry Department, Indiana University 800 E. Kirkwood Avenue, Bloomington Indiana 47405, United States

**ABSTRACT:** Heat capacities have been measured as a function of temperature for size-selected gallium cluster cations with between 60 and 183 atoms. Almost all clusters studied show a single peak in the heat capacity that is attributed to a melting transition. The peaks can be fit by a two-state model incorporating only fully solid-like and fully liquid-like species, and hence no partially melted intermediates. The exceptions are  $\text{Ga}_{90}^+$ , which does not show a peak, and  $\text{Ga}_{80}^+$  and  $\text{Ga}_{81}^+$ , which show two peaks. For the clusters with two peaks, the lower temperature peak is attributed to a structural transition. The melting temperatures for clusters with less than 50 atoms have previously been shown to be hundreds of degrees above the bulk melting point. For clusters with more than 60 atoms the melting temperatures decrease, approaching the bulk value (303 K) at around 95 atoms, and then show several small upward excursions with increasing cluster size. A plot of the latent heat against the entropy change for melting reveals two groups of clusters: the latent heats and entropy changes for clusters with less than 94 atoms are distinct from those for clusters with more than 93 atoms. This observation suggests that a significant change in the nature of the bonding or the structure of the clusters occurs at 93–94 atoms. Even though the melting temperatures are close to the bulk value for the larger clusters studied here, the latent heats and entropies of melting are still far from the bulk values.



## INTRODUCTION

It has been more than a century since Pawlow predicted that the melting temperatures of small particles were lower than the bulk melting point.<sup>1</sup> The melting temperature depression is a thermodynamic consequence of the change in the surface to volume ratio that occurs with decreasing particle size and has now been confirmed experimentally in a number of studies.<sup>2–10</sup> However, in the cluster-size regime (tens to hundreds of atoms) physical properties are known to change dramatically with the addition or subtraction of a single atom.<sup>11</sup> The melting temperatures of size-selected metal clusters have been investigated by calorimetric methods where the heat capacity is measured as a function of temperature, and the melting temperature determined from a peak in the heat capacity due to the latent heat.<sup>12–14</sup> Sodium and aluminum clusters have been the most widely studied, and for these metals the clusters have depressed melting temperatures with large size-dependent fluctuations.<sup>12,15–25</sup> In some cases, fluctuations of hundreds of degrees occur with the addition or removal of a single atom.<sup>26</sup>

Not all metal clusters have depressed melting temperatures. Evidence for elevated melting temperatures was first obtained for tin clusters.<sup>27,28</sup> However, in this case, the evidence was indirect because tin clusters dissociate before they melt. Subsequent calorimetry measurements for small gallium clusters showed that their melting temperatures were elevated above the bulk value.<sup>13,29–32</sup> Gallium droplets (with an average size of 0.39  $\mu\text{m}$ ) dispersed in epoxy have been shown to supercool to around 150 K.<sup>33</sup> Once frozen, they melt upon rewarming at around 254 K. The most stable phase of gallium at room temperature and pressure is the  $\alpha$ -phase, which melts at 303 K. However, the droplets were found to freeze into the  $\beta$ -phase, which normally melts into a supercooled liquid at 257

K.<sup>34</sup> Thus, the melting point depression is only a few kelvin, but in line with expectations for these relatively large particles. This result shows that large gallium particles have depressed melting points, in agreement with the thermodynamic arguments of Pawlow.

The gallium particles discussed above freeze into the  $\beta$ -phase. Freezing into the  $\alpha$ -phase involves an expansion, so this would be disfavored for particles embedded in a matrix. However, nanoparticles on surfaces have also been found to freeze into the  $\beta$ -phase.<sup>35</sup> Clearly there must be some other factor (perhaps the complexity of the  $\alpha$ -phase) that favors freezing into the  $\beta$ -phase in small particles. The  $\alpha$ -phase has a complicated orthorhombic structure with eight atoms in the unit cell. Each atom has one nearest neighbor at 2.44 Å and six next-nearest neighbors arranged in pairs at 2.69–2.71 Å. The structure has been described as a molecular metal composed of dimers perpendicular to the metallic bonding plane.<sup>36–38</sup>

Recent results obtained using wave-function-based methods and density functional theory (DFT) suggest that some small neutral and positively charged gallium clusters (up to  $\text{Ga}_8$ ) may have dimer pairings similar to the bulk.<sup>37</sup> However, the elevated melting temperatures for gallium clusters with less than 55 atoms implies that the nature of the bonding in the clusters is very different from that in the bulk.<sup>32,39–42</sup> While the fact that there must be a difference seems settled, there has been disagreement over how the bonding differs. Chacko et al. originally suggested that the bonding in the clusters was more covalent than the bulk,<sup>40</sup> while Núñez et al. suggest the bonding

Received: April 3, 2014

Revised: May 29, 2014

Published: June 30, 2014

in the clusters is more metallic.<sup>41</sup> Steenbergen et al. reach the same conclusion.<sup>42</sup> It has also been suggested that the higher-than-bulk melting temperature of the gallium clusters may not be the anomaly it seems; it is actually the low melting temperature of the pseudocovalent bulk that is the real anomaly (at least from the perspective of the periodic table).<sup>37,41</sup>

Calorimetry measurements for small gallium clusters have revealed substantial size-dependent variations in the size and width of the peak in the heat capacity. Some clusters have intense, narrow peaks indicating a well-defined melting transition with a relatively large latent heat, while for others, melting (detected by ion mobility measurements) appears to occur without a peak in the heat capacity.<sup>29–32</sup> For a cluster to melt without a latent heat, the solid and liquid phases must have similar energies. This type of transition is usually described as second-order<sup>31</sup> in contrast to the first-order transitions that occur with a latent heat.

The origin of the different types of melting behavior described above has been investigated by Joshi et al. using *ab initio* molecular dynamic simulations for Ga<sub>30</sub> and Ga<sub>31</sub>.<sup>43</sup> In the experiments, Ga<sub>31</sub><sup>+</sup> shows a well-defined peak in the heat capacity, whereas for Ga<sub>30</sub><sup>+</sup> the peak is broad and ill-defined.<sup>30</sup> Joshi et al. found that Ga<sub>30</sub> has a disordered or amorphous ground state that results in a broad peak in the heat capacity without a defined melting transition. Conversely, Ga<sub>31</sub> has an “ordered” ground state that results in a sharp, well-defined phase transition. The ordered ground state of Ga<sub>31</sub> has an energy considerably below that of the low-energy amorphous structures. In a related study, the structures of Ga<sub>17</sub><sup>+</sup> and Ga<sub>20</sub><sup>+</sup> were investigated.<sup>32</sup> Ga<sub>20</sub><sup>+</sup> has a well-defined melting transition, whereas the melting transition for Ga<sub>17</sub><sup>+</sup> is poorly defined. Differences in bond-length distributions, isomer distributions, coordination numbers, and nature of the bonding were investigated. The authors concluded that there is a strong correlation between the ground state geometry and the nature of the melting transition. A symmetric well-ordered ground state leads to a distinct peak in the heat capacity, while amorphous or disordered ground states lead to melting without a peak.<sup>32</sup> The relationship between local-order and size-dependent melting behavior is not exclusive to gallium clusters; a correlation has also been identified in small sodium clusters.<sup>44,45</sup> Susan et al. have found that the melting temperature for gallium clusters with 31–48 atoms is correlated with the structure, with more spherical geometries leading to a higher melting temperature.<sup>46</sup> Hence, according to this work, the variation in the melting temperature has a structural origin.

In this article, we present measurements of heat capacities for gallium clusters with between 60 and 183 atoms. This work compliments the earlier experimental studies that extended only up to Ga<sub>55</sub><sup>+</sup>.<sup>30</sup> The results we present here should catalyze more theoretical studies of phase transitions in gallium clusters.

## ■ EXPERIMENTAL METHODS

A detailed description of the instrument and experimental methods can be found elsewhere.<sup>47</sup> Briefly, a XeF excimer laser is used to ablate a high purity (99.999%) liquid gallium target in a continuous flow (~400 sccm) of high purity helium. A liquid target continuously fills in the hole generated by laser ablation and maintains a more pristine and uniform surface than can be obtained with a solid target. Both of these factors increase the signal stability.<sup>48</sup> The source region is cooled to around 273 K to encourage the ablated gallium atoms to condense into clusters.

After generation, the clusters enter a 10 cm long temperature-variable extension where the temperature is set to  $\pm 2$  K by a programmable microcontroller. In the extension, the clusters undergo enough collisions to be fully thermalized. After exiting the extension, positively charged clusters are accelerated and focused into the first of two quadrupole mass filters. In the quadrupole, a single cluster size is isolated on the basis of its  $m/z$  ratio. The size-selected clusters are then focused by an Einzel lens into a high pressure collision cell filled with 0.400 Torr of neon. The translational energy of the ions entering the collision cell is controlled by the potential difference between the exit plate of the temperature-variable extension on the source and the entrance plate of the collision cell.

As the clusters enter the collision cell they undergo many collisions with the gas inside. A small fraction of the ions' translational energy is converted into internal energy in each collision, and the ions' translational energy is eventually thermalized. If the cluster ions' initial translational energy is high enough, they are heated to the point where they dissociate. After their translational energy is thermalized, any undissociated parent cluster ions and product ions are drawn across the collision cell by a weak electric field. Some of these ions exit the collision cell through a small aperture. They are then accelerated and focused into the second quadrupole mass filter. The RF and DC voltages supplied to this quadrupole are scanned to transmit ions with different  $m/z$  and measure the  $m/z$  spectrum. The ions that are transmitted through the mass filter are detected by an off-axis collision dynode and a dual microchannel plate assembly.

Helium was used as the collision gas in our previous calorimetry studies of gallium clusters. However, we found that the larger clusters studied here were not being completely thermalized by helium. Consequently, they exited the collision cell and entered the second quadrupole mass filter with excess kinetic energy. The excess kinetic energy degraded the  $m/z$  resolution of the quadrupole. Also, incomplete thermalization of the ions may cause the amount of dissociation to be underestimated, leading to erroneous heat capacity values. Using a heavier collision gas, neon, solved this problem.

The measured mass spectra show that the gallium clusters studied here dissociate by sequential loss of gallium atoms. The spectra were analyzed to determine the degree of dissociation. Measurements were made at six different initial translational energies that lead to around 50% dissociation. A linear regression was used to determine the ion energy necessary for 50% dissociation of the parent cluster (TES0%D). If the TES0%D values are plotted as a function of the temperature of the temperature-variable extension, a step indicates a sudden change in internal energy that is a consequence of a phase transition. The derivative of this plot with respect to temperature is proportional to the heat capacity. The proportionality constant is related to fraction of the ions translational energy converted into internal energy, which is obtained from an impulsive collision model.<sup>49,50</sup> The phase transition is indicated by a peak in the plot of the heat capacity against temperature and the area under the peak is the latent heat.

## ■ RESULTS

Figure 1 shows heat capacities measured as a function of temperature for Ga<sub>*n*</sub><sup>+</sup> where *n* (the number of atoms in the cluster) is 61, 80, 92, and 94. The heat capacities are plotted in classical units,  $3Nk_B$ , where  $k_B$  is the Boltzmann constant and

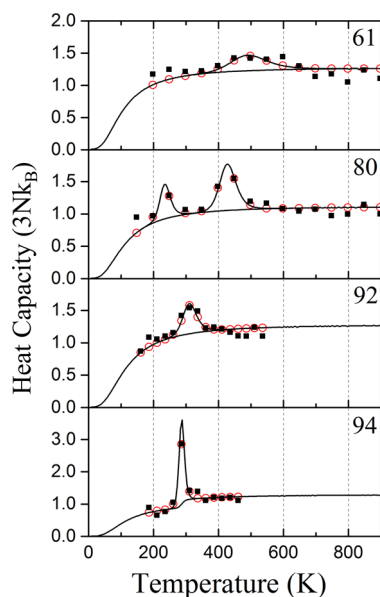


**Figure 1.** Plots of heat capacity versus temperature for  $\text{Ga}_{61}^+$ ,  $\text{Ga}_{80}^+$ ,  $\text{Ga}_{92}^+$ , and  $\text{Ga}_{94}^+$ . The heat capacities are in classical units of  $3Nk_B$ , where  $3N = 3n - 6 + 3/2$ ,  $n$  is the number of atoms in the cluster, and  $k_B$  is the Boltzmann constant. The black squares are the measured values with  $\Delta T = 25$  K and  $\Delta T = 50$  K. The open-red circles are fits to the experimental data using the two- and three-state models described in the text with the same temperature intervals as used in the experiments. The solid black line shows the heat capacities calculated with the model using  $\Delta T = 5$  K.

$3N = (3n - 6 + 3/2)$ , which includes both the vibrational and rotational contributions to the heat capacity. The black squares in Figure 1 are the experimental values measured with  $\Delta T = 25$  or  $50$  K. Measurements were initially performed for all clusters with  $\Delta T = 50$  K. Additional measurements were performed for many clusters with  $\Delta T = 25$  K to better resolve the features in the heat capacity. The smaller temperature interval was especially important for clusters with more than 93 atoms, where the peak in the heat capacity is narrow. Most clusters have three data points across the peak. All data points (both  $\Delta T = 25$  and  $\Delta T = 50$  K) are an average of at least three measurements.

The heat capacity plot for  $\text{Ga}_{61}^+$  shows a broad low intensity peak centered around  $500$  K. The plot for  $\text{Ga}_{80}^+$  is unusual in that there appear to be two peaks in the heat capacity, one centered at around  $225$  K and the other at around  $425$  K.  $\text{Ga}_{81}^+$  is the only other cluster examined here that clearly shows two peaks.  $\text{Ga}_{92}^+$  in Figure 1 shows a single sharp peak centered at around  $300$  K, and  $\text{Ga}_{94}^+$  shows a substantially sharper peak centered at around the same temperature. Note that the vertical scale in Figure 1 is larger for  $\text{Ga}_{94}^+$  than for the other clusters. The area under the peaks is the latent heat, and as we will see below, the latent heat for  $\text{Ga}_{94}^+$  is substantially larger than for  $\text{Ga}_{92}^+$ .

The open red circles in Figure 1 are the fit to the experimental data from either a two-state or three-state model. These models are described in detail elsewhere.<sup>25</sup> Briefly, the two-state model assumes that only fully liquid-like and fully solid-like clusters exist. At the phase transition there is a dynamic phase coexistence, where each cluster switches back and forth between being fully liquid-like and fully solid-like. This behavior is different from the bulk where partial melting occurs and the two phases coexist in contact. In the two-state

model, the fractions of liquid and solid clusters present at any given temperature are determined by an equilibrium constant. The contribution to the heat capacity due to the phase transition is obtained from the latent heat multiplied by the change in the fraction of liquid clusters over the relevant temperature range ( $\Delta T = 25$  and  $50$  K in this work). This contribution from the phase transition is added to the underlying heat capacity of the solid-like and liquid-like clusters, which is obtained from a modified Debye model.<sup>51</sup> The modified Debye model accounts for the finite size of the clusters by including a low frequency cutoff in addition to the expected high frequency cutoff. The overall model is fit to the experimental data by adjusting the latent heat and melting temperature using a least-squares criterion. We also account for the fact that the solid-like and liquid-like clusters may have different underlying heat capacities. Examples of the fits obtained with the two-state model are shown by the open red circles in Figure 1 for  $\text{Ga}_{61}^+$ ,  $\text{Ga}_{92}^+$ , and  $\text{Ga}_{94}^+$ . The melting temperatures and latent heats deduced from the fits are presented below.

In the three-state model it is assumed that there is an intermediate between the fully solid and fully liquid clusters.<sup>25</sup> The nature of the intermediate is not specified. It could result from partial melting (perhaps surface melting) or a geometric rearrangement of the solid phase. In the three-state model, two equilibrium constants relate the relative abundances of the solid-like, intermediate, and liquid-like clusters. In addition, there are enthalpy changes associated with conversion of the solid-like to intermediate and the intermediate to liquid-like. The enthalpy changes and transition temperatures are obtained by optimizing the fit of the model to the measurements using a least-squares criterion. The three-state model was only used for clusters with 80 and 81 atoms, the only ones studied that clearly had two maxima in the heat capacity.

The optimized fits to the experimental measurements with the two-state and three-state models provide values for the transition temperatures and enthalpies that we discuss further below. The solid black lines in Figure 1 were calculated using the two- and three-state models and the transition temperatures and enthalpies obtained from the fits to the measured values, but with  $\Delta T = 5$  K. A temperature increment of  $\Delta T = 5$  K is considerably smaller than the  $\Delta T = 25$  and  $50$  K that were used in the experiments. When the peaks in the heat capacity are broad, the solid black lines (calculated with  $\Delta T = 5$  K) go through the red circles (calculated with  $\Delta T = 25$  or  $50$  K), which indicates that the  $\Delta T$  used in the experiments ( $25$  or  $50$  K) is small enough for the measurements to provide a true representation of the peak in the heat capacity. However, when the peaks are very narrow the agreement between the red points ( $\Delta T = 25$  K) and the line ( $\Delta T = 5$  K) is not so good. This indicates that it would be beneficial to use a smaller temperature increment to provide a more accurate reproduction of the heat capacity peak. However, using a smaller  $\Delta T$  is not without cost because it leads to smaller and less reliable changes in the internal energy. The uncertainty in the temperature of the extension also becomes more significant as the  $\Delta T$  is reduced. We decided that it was probably better to use the larger  $\Delta T$  values and obtain a less faithful representation of the peak because the models used to fit the measurements can compensate for the larger  $\Delta T$ . Note that using the larger  $\Delta T$  does not compromise the determination of the transition enthalpies. Although the transition enthalpies are given by the areas under the peaks in the heat capacity, in the

experiment we actually measure the internal energy (the integral of the heat capacity with respect to temperature) where the latent heat is manifested as a step. The height of the step gives the latent heat, and the sharpness of the step does not influence its height.

For all of the clusters where peaks were observed in the heat capacities, the results were analyzed using either the two- or three-state models where the melting temperatures and latent heats are fitting parameters. The melting temperatures obtained from the fits are shown in Figure 2. In addition to the clusters

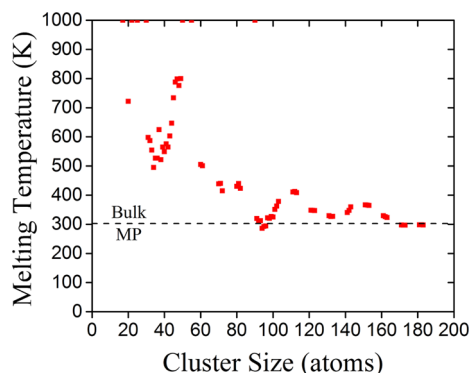


**Figure 2.** Melting temperatures (determined from the fits to the peaks in the heat capacities) plotted against the number of atoms in each cluster. The melting temperatures shown for clusters with <60 atoms were obtained from previously reported work.<sup>29–32</sup>

studied here (clusters with between 60 and 183 atoms), we also show in Figure 2 the melting temperatures obtained in earlier work for clusters with 17–55 atoms.<sup>29–32</sup> Some clusters do not show a peak in their heat capacity. This behavior is indicated in Figure 2 by a point at the top of the melting temperature axis to show that the cluster was studied but a peak was not detected.

The absence of a peak is fairly common for the smaller clusters studied previously, where a peak is absent for clusters with 17, 22, 25, 30, 50, and 55 atoms. However, only one of the larger clusters studied did not show a peak:  $\text{Ga}_{90}^+$ . As noted above,  $\text{Ga}_{80}^+$  and  $\text{Ga}_{81}^+$  show more than one peak in the heat capacity, the first peak at approximately 200 K lower than the second. For these clusters we show in Figure 2 the temperature associated with the higher temperature peak. We assume that this is the melting transition. If the lower temperature peak was due to melting, then the higher temperature one could only be due to a liquid–liquid phase transition. A transition between two distinct liquid forms is rare in pure substances and invariably occurs at elevated pressures,<sup>52–54</sup> so it seems unlikely that the higher temperature peak observed for  $\text{Ga}_{80}^+$  and  $\text{Ga}_{81}^+$  results from such a process.

The measured melting temperatures (Figure 2) show an overall decrease with increasing cluster size, but substantial local fluctuations also exist. There are local maxima in the melting temperatures for clusters with around 50, 80, 105, and 145 atoms. The dashed horizontal line in the figure shows the melting point of bulk gallium (303 K). As noted elsewhere the small clusters have melting points that are considerably above the bulk value. The melting temperatures first drop below the bulk value for clusters with around 95 atoms and then rise again, dropping below the bulk melting point again at around 170 atoms. Overall, the melting temperatures vary by over 500 K for gallium clusters with between 20 and 183 atoms.

The upper panels in Figure 3 show the latent heats determined from the measurements by fitting them with the two-state and three-state models. For  $\text{Ga}_{80}^+$  and  $\text{Ga}_{81}^+$  (the only clusters showing two peaks, and hence the only ones fit with the three-state model) we show the enthalpy change associated with the higher temperature transition (for reasons already discussed above). Clusters that were studied, but for which no clear peak in the heat capacity was observed, are indicated by a

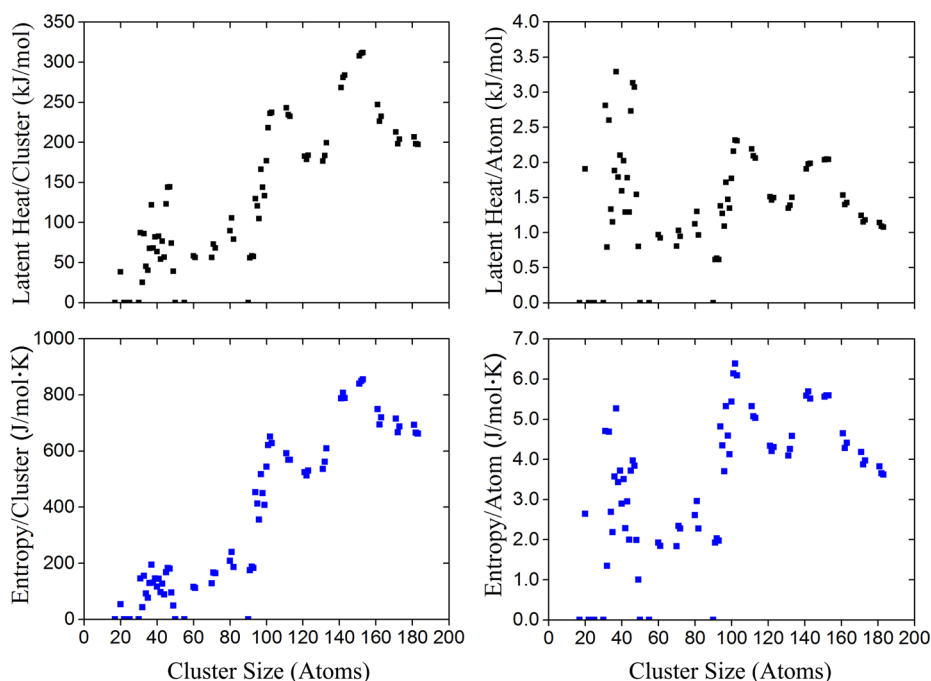


**Figure 3.** (Top) Plots of the latent heat per cluster (left) and latent heat per atom (right) against the number of atoms in the each cluster. (Bottom) Plots of the change in entropy per cluster (left) and the change in entropy per atom (right) against the number of atoms in each cluster. The results for clusters with <60 atoms are from previously reported work.<sup>29–32</sup>

point on the lower axis of the plot. For comparison, we have included the latent heats obtained in earlier work for clusters with 17–55 atoms.<sup>29–32</sup> The plot in the upper left of Figure 3 shows the latent heat per cluster, and the plot in the upper right shows the latent heat per atom. The latent heats of the smaller clusters show large fluctuations with particularly large latent heats being observed for some clusters (20, 31, 33, 37, 45, 46, and 47 atoms). For the larger clusters there are broad local maxima in the latent heats centered around 105 and 145 atoms. The latent heats per atom range up to around 3.5 kJ/mol. The latent heat (per atom) for the melting of bulk gallium is 5.59 kJ/mol, so the latent heats of the clusters are all considerably below the bulk value. Furthermore, the latent heats per atom for the larger clusters in Figure 3 seem to be trending down and moving further away from the bulk value as the cluster size increases.

The entropy change for a first-order phase transition can be deduced from  $\Delta S_m = \Delta H_m/T_m$ , where  $\Delta H_m$  is the latent heat and  $T_m$  is the melting temperature. The entropy changes deduced using this equation are shown in the lower panels of Figure 3. The entropy changes per cluster are shown on the left, and the entropy changes per atom are on the right. The entropy change for the melting of bulk gallium is 18.4 J/mol·K, which is considerably larger than the values determined for the clusters (which are all below 7 J/mol·K). The size-dependent behavior of the entropies is similar to the latent heats: rapid and erratic size-dependent fluctuations for the small clusters and broad oscillations for the larger ones with maxima around 100 and 145 atoms.

## DISCUSSION

A peak in the heat capacity indicates a phase transition. For a macroscopic crystal the peak due to melting is a  $\delta$ -function and there is a single melting point. Metal clusters are expected to exhibit broader transitions due to finite size effects.<sup>55–57</sup> They are also expected to display a dynamic phase coexistence where the clusters at the melting temperature flip back and forth between fully liquid-like and fully solid-like.<sup>58,59</sup> This contrasts with the behavior of the macroscopic crystals where the two phases coexist in contact at the melting point. In the two-state model used to analyze the measurements for most of the clusters, the melting transition is described by an equilibrium, and so we can write

$$\ln K = -\frac{\Delta H}{RT} + \frac{\Delta S}{R} = -\frac{\Delta H}{RT} + \frac{\Delta H}{RT_m}$$

where  $K$  is the equilibrium constant,  $\Delta H$  and  $\Delta S$  are the enthalpy and entropy changes for melting, and  $T_m$  is the melting temperature. The width of the transition is determined by the temperature change required to swing  $K$  from a small value (say 0.1) to a large value (say 10.0). This width is governed by the enthalpy change between the solid-like and liquid-like clusters (and to a lesser extent, the melting temperature). As the enthalpy change increases, the transition is expected to become narrower. The two-state model reproduces the widths of the transitions for the smaller clusters studied here and accounts for the decrease in the width of the transition that occurs as the enthalpy change increases. When the enthalpy change becomes large, it is not possible to judge how well the model fits the width of the peak because the width is influenced by the  $\Delta T$  used in the measurements (see Results section).

Most gallium clusters exhibit a single peak in heat capacity.  $\text{Ga}_{80}^+$  and  $\text{Ga}_{81}^+$  exhibit two peaks and were fit with a three-state model. A bimodal peak (i.e., two poorly resolved peaks) was observed in previous work for  $\text{Ga}_{49}^+$ . Bimodal peaks have also been observed for some aluminum clusters. Both premelting, with a small low temperature feature (for example,  $\text{Al}_{51}^+$  and  $\text{Al}_{52}^+$ ),<sup>20</sup> and postmelting, with a small high temperature feature (for example,  $\text{Al}_{61}^+$  and  $\text{Al}_{83}^+$ ),<sup>60</sup> were observed. This behavior has often been attributed to different parts of the cluster melting at different temperatures; hence it may be related to surface premelting that occurs with bulk materials. Simulations for sodium clusters have shown both premelting and postmelting features.<sup>61</sup> For  $\text{Na}_{139}^+$ , premelting features were attributed to anharmonic effects and the diffusion of surface vacancies, while for icosahedral  $\text{Na}_{147}^+$  the two outer layers melt and are liquid while the inner 13-atom icosahedron remains solid up to 40 K above which the surface melts. In the case of  $\text{Al}_{115}^+$ ,  $\text{Al}_{116}^+$ , and  $\text{Al}_{117}^+$  fully resolved peaks separated by around 150 K were found.<sup>23</sup> It is difficult to imagine liquid and solid portions of the clusters coexisting over such an extended temperature range. Annealing experiments were consistent with the view that the lower temperature peak is due to a solid-to-solid transition (i.e., a structural transition). In the case of  $\text{Ga}_{80}^+$  and  $\text{Ga}_{81}^+$  studied here, the peaks are close to 200 K apart, and the most likely explanation is that the lower temperature peak is due to a structural transition. Note that a peak in the heat capacity indicates that the transition is to a higher enthalpy (and higher entropy) structure. For a number of aluminum clusters we also observed dips in the heat capacity before the melting transition. A dip indicates a transition to a lower enthalpy (and lower entropy) structure. We did not observe any significant dips for the gallium clusters studied here.

While small metal particles are expected to have depressed melting temperatures,<sup>1</sup> small gallium clusters have melting temperatures considerably above the bulk value (see Figure 2).<sup>29–32</sup> The elevated melting temperatures have been attributed to the clusters having different bonding and structures than the bulk.<sup>40,41</sup> For larger clusters the melting temperatures drop precipitously, reaching the bulk value (303 K) at around  $\text{Ga}_{90}^+$ . While we use the melting point of the  $\alpha$ -phase (303 K) as the reference for bulk properties, it could be argued that the melting point of the  $\beta$ -phase (257 K) provides a better reference for the clusters studied here. It is doubtful that clusters with less than 200 atoms could adopt the complicated  $\alpha$ -phase structure of the bulk material. If we use the  $\beta$ -phase as a reference, the melting temperatures of the clusters are still considerably above the bulk value, despite the sharp drop that occurs for clusters with more than 50 atoms. It is not yet known whether this sharp drop in the melting temperature has a structural origin. As we discuss below, the latent heat and entropy of melting are still far from their bulk values even for the largest clusters studied here, so it would be reckless to interpret the decrease in the melting temperatures as due to the evolution of bulk-like structures. The size-dependent fluctuations in the melting temperatures also diminish with increasing cluster size, and above  $\text{Ga}_{90}^+$  there are just gentle oscillations.

One cluster in the size range examined here,  $\text{Ga}_{90}^+$ , did not show a peak in the heat capacity. The most likely explanation for this behavior is that the solid-like state is disordered with similar enthalpy and entropy as the liquid-like state, so when the cluster melts there is no peak in the heat capacity, the cluster analogue of a second-order phase transition. This view is

consistent with theoretical studies where the melting behavior of  $\text{Ga}_{17}^+$  was compared with  $\text{Ga}_{20}^+$  and  $\text{Ga}_{30}$  was compared with  $\text{Ga}_{31}$ .<sup>32,43</sup>  $\text{Ga}_{17}^+$  and  $\text{Ga}_{30}^+$  do not show a peak in their heat capacities, whereas both  $\text{Ga}_{20}^+$  and  $\text{Ga}_{31}^+$  show peaks. For the clusters that did not show peaks, the theoretical studies found a disordered solid and for those that show a well-defined peak the ground state was more ordered.

The latent heats and entropies for melting are shown in Figure 3. At the upper end of the size range studied here both quantities are a substantial distance from their bulk values. For example, the latent heats are around 1.0 kJ/mol compared to the bulk value of 5.59 kJ/mol, and the entropies are around 3.5 J/mol·K compared to the bulk value of 18.4 J/mol·K. So even though the melting temperatures are close to the bulk value, the thermodynamic quantities responsible for the phase transition are not. The only reason that the melting temperatures are close to the bulk value is that both the latent heat and the entropy deviate from their respective bulk values by about the same proportion. Inspection of Figure 3 shows that there is a correlation between the enthalpy and entropy changes. Such a correlation has been noted before for both sodium and aluminum clusters.<sup>17,26</sup> A correlation between the latent heats (enthalpies) and entropies means that substantial changes in the latent heats do not lead to large changes in the melting temperatures. Without this correlation, the fluctuations in the melting temperatures would be much larger.

To further examine the correlation between the latent heats and the entropies, Figure 4 shows the latent heats per atom

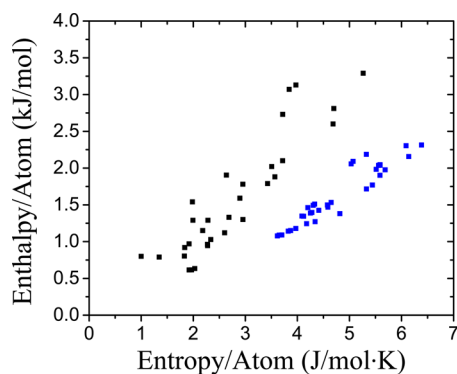


**Figure 4.** Plot of the enthalpy change per atom for melting against the entropy change per atom for melting. The results for clusters with  $\leq 93$  atoms are shown in black, and the results for clusters with  $\geq 94$  atoms are shown in blue.

plotted against the entropy changes per atom. The points appear to fall into two groups: a group with the larger latent heats per atom, the more diffuse group, and a tighter group with smaller latent heats per atom. The diffuse group contains clusters with up to 93 atoms. The tighter group contains clusters with more than 93 atoms. These results suggest that a fundamental change in the nature of the clusters occurs at 93–94 atoms. Inspection of Figure 3 reveals that both the latent heats and the entropy changes undergo substantial jumps in their values at this point. Our results do not provide any insight into the nature of the change that occurs for clusters with 93–94 atoms. However, the most likely explanation is that there is a fundamental change in the nature of the bonding or the geometry of the clusters at this point.

## AUTHOR INFORMATION

### Corresponding Author

\*E-mail: mfj@indiana.edu.

### Notes

The authors declare no competing financial interest.

## ACKNOWLEDGMENTS

We gratefully acknowledge the support of the National Science Foundation through grant number 0911462.

## REFERENCES

- (1) Pawlow, P. Über die Abhängigkeit des Schmelzpunktes von der Oberflächenenergie eines Festen Körpers. *Z. Phys. Chem.* **1909**, *65*, 1–35.
- (2) Takagi, M. Electron-Diffraction Study of Liquid-Solid Transition of Thin Metal Films. *J. Phys. Soc. Jpn.* **1954**, *9*, 359–363.
- (3) Peppiatt, S. J.; Sambles, J. R. The Melting of Small Particles. I. Lead. *Proc. R. Soc. London A* **1975**, *345*, 387–399.
- (4) Peppiatt, S. J. The Melting of Small Particles. II. Bismuth. *Proc. R. Soc. London A* **1975**, *345*, 401–412.
- (5) Buffat, P.; Borel, J. P. Size Effect on the Melting Temperature of Gold Particles. *Phys. Rev. A* **1976**, *13*, 2287–2298.
- (6) Couchman, P. R.; Jesser, W. A. Thermodynamic Theory of Size Dependence of Melting Temperature in Metals. *Nature* **1977**, *269*, 381–483.
- (7) Borel, J. P. Thermodynamical Size Effect and the Structure of Metallic Clusters. *Surf. Sci.* **1981**, *106*, 1–9.
- (8) Ross, J.; Andres, R. P. Melting Temperature of Small Clusters. *Surf. Sci.* **1981**, *106*, 11–17.
- (9) Lai, S. L.; Guo, J. Y.; Petrova, V.; Ramanath, G.; Allen, L. H. Size-Dependent Melting Properties of Small Tin Particles: Nanocalorimetric Measurements. *Phys. Rev. Lett.* **1996**, *77*, 99–102.
- (10) Bottani, C. E.; Bassi, A. L.; Tanner, B. K.; Stella, A.; Tognini, P.; Cheyssac, P.; Kofman, R. Melting in Metallic Sn Nanoparticles Studied by Surface Brillouin Scattering and Synchrotron X-Ray Diffraction. *Phys. Rev. B* **1999**, *59*, R15601–R15604.
- (11) de Heer, W. A. The Physics of Simple Metal Clusters: Experimental Aspects and Simple Models. *Rev. Mod. Phys.* **1993**, *65*, 611–676.
- (12) Schmidt, M.; Kusche, R.; Kronmüller, W.; von Issendorff, B.; Haberland, H. Experimental Determination of the Melting Point and Heat Capacity for a Free Cluster of 139 Sodium Atoms. *Phys. Rev. Lett.* **1997**, *79*, 99–102.
- (13) Breaux, G. A.; Benirschke, R. C.; Sugai, T.; Kinnear, B. S.; Jarrold, M. F. Hot and Solid Gallium Clusters: Too Small to Melt. *Phys. Rev. Lett.* **2003**, *91*, 215508.
- (14) Chirof, F.; Feiden, P.; Zamith, S.; Labastie, P.; L'Hermite, J. M. A Novel Experimental Method for the Measurement of the Caloric Curves of Clusters. *J. Chem. Phys.* **2008**, *129*, 164514.
- (15) Schmidt, M.; Kusche, R.; Hippler, T.; Donges, J.; Kronmüller, W.; von Issendorff, B.; Haberland, H. Negative Heat Capacity for a Cluster of 147 Sodium Atoms. *Phys. Rev. Lett.* **2001**, *86*, 1191–1194.
- (16) Schmidt, M.; Haberland, H. Phase Transitions in Clusters. *C. R. Phys.* **2002**, *3*, 327–340.
- (17) Schmidt, M.; Donges, J.; Hippler, T.; Haberland, H. Influence of Energy and Entropy on the Melting of Sodium Clusters. *Phys. Rev. Lett.* **2003**, *90*, 103401.
- (18) Haberland, H.; Hippler, T.; Donges, J.; Kostko, O.; Schmidt, M.; von Issendorff, B. Melting of Sodium Clusters: Where Do the Magic Numbers Come From? *Phys. Rev. Lett.* **2005**, *94*, 035701.
- (19) Hock, C.; Strassburg, S.; Haberland, H.; von Issendorff, B.; Aguado, A.; Schmidt, M. Melting Point Depression by Small Insoluble Impurities: A Finite Size Effect. *Phys. Rev. Lett.* **2008**, *101*, 023401.
- (20) Breaux, G. A.; Neal, C. M.; Cao, B.; Jarrold, M. F. Melting, Pre-Melting, and Structural Transitions in Size-Selected Aluminum Clusters with Around 55 Atoms. *Phys. Rev. Lett.* **2005**, *94*, 173401.

- (21) Neal, C. M.; Starace, A. K.; Jarrold, M. F.; K, J.; Krishnamurty, S.; Kanhere, D. G. Melting of Aluminum Cluster Cations with 31–48 Atoms: Experiment and Theory. *J. Phys. Chem. C* **2007**, *111*, 17788–17794.
- (22) Starace, A. K.; Neal, C. M.; Cao, B.; Jarrold, M. F.; Aguado, A.; Lopez, J. M. Correlation Between the Latent Heats and Cohesive Energies of Metal Clusters. *J. Chem. Phys.* **2008**, *129*, 144702.
- (23) Cao, B.; Starace, A. K.; Judd, O. H.; Bhattacharyya, I.; Jarrold, M. F. Metal Clusters with Hidden Ground States: Melting and Structural Transitions in  $Al_{115}^+$ ,  $Al_{116}^+$ , and  $Al_{117}^+$ . *J. Chem. Phys.* **2009**, *131*, 124305.
- (24) Starace, A. K.; Neal, C. M.; Cao, B.; Jarrold, M. F.; Aguado, A.; López, J. M. Electronic Effects on Melting: Comparison of Aluminum Cluster Anions and Cations. *J. Chem. Phys.* **2009**, *131*, 044307.
- (25) Starace, A. K.; Cao, B.; Judd, O. H.; Bhattacharyya, I.; Jarrold, M. F. Melting of Size-Selected Aluminum Nanoclusters with 84–128 Atoms. *J. Chem. Phys.* **2010**, *132*, 034302.
- (26) Aguado, A.; Jarrold, M. F. Melting and Freezing of Metal Clusters. *Annu. Rev. Phys. Chem.* **2011**, *62*, 151–172.
- (27) Shvartsburg, A. A.; Jarrold, M. F. Solid Clusters Above the Bulk Melting Point. *Phys. Rev. Lett.* **2000**, *85*, 2530–2532.
- (28) Breaux, G. A.; Neal, C. M.; Cao, B.; Jarrold, M. F. Tin Clusters That Do Not Melt: Calorimetry Measurements up to 650 K. *Phys. Rev. B* **2005**, *71*, 073410.
- (29) Breaux, G.; Benirschke, R.; Sugai, T.; Kinnear, B.; Jarrold, M. F. Hot and Solid Gallium Clusters: Too Small to Melt. *Phys. Rev. Lett.* **2003**, *91*, 215508.
- (30) Breaux, G.; Hillman, D.; Neal, C.; Benirschke, R.; Jarrold, M. F. Gallium Cluster “Magic Melters”. *J. Am. Chem. Soc.* **2004**, *126*, 8628–8629.
- (31) Breaux, G.; Cao, B.; Jarrold, M. F. Second-Order Phase Transitions in Amorphous Gallium Clusters. *J. Phys. Chem. B* **2005**, *109*, 16575–16578.
- (32) Krishnamurty, S.; Chacko, S.; Kanhere, D.; Breaux, G.; Neal, C. M.; Jarrold, M. F. Size-Sensitive Melting Characteristics of Gallium Clusters: Comparison of Experiment and Theory for  $Ga_{17}^+$  and  $Ga_{20}^+$ . *Phys. Rev. B* **2006**, *73*, 045406.
- (33) Cicco, A. D. Phase Transitions in Confined Gallium Droplets. *Phys. Rev. Lett.* **1998**, *81*, 2942–2945.
- (34) Bosio, L.; Defrain, A.; Curien, H.; Rimsky, A. Structure Cristalline du Gallium  $\beta$ . *Acta Crystallogr. B* **1969**, *25*, 995.
- (35) Pochon, S.; MacDonald, K. F.; Knize, R. J.; Zheludev, N. I. Phase Coexistence in Gallium Nanoparticles Controlled by Electron Excitation. *Phys. Rev. Lett.* **2004**, *92*, 145702.
- (36) Yang, J.; Tse, J.; Iitaka, T. First-Principle Study of Liquid Gallium at Ambient and High Pressure. *J. Chem. Phys.* **2011**, *135*, 044507.
- (37) Gaston, N.; Parker, A. On the Bonding of  $Ga_2$ , Structures of  $Ga_n$  clusters and the Relation to the Bulk Structure of Gallium. *Chem. Phys. Lett.* **2011**, *501*, 375–378.
- (38) Drebov, N.; Weigend, F.; Ahlrichs, R. Structures and Properties of Neutral Gallium Clusters: A Theoretical Investigation. *J. Chem. Phys.* **2011**, *135*, 044314.
- (39) Joshi, K.; Kanhere, D.; Blundell, S. Abnormally High Melting Temperature of the  $Sn_{10}$  Cluster. *Phys. Rev. B* **2002**, *66*, 155329.
- (40) Chacko, S.; Joshi, K.; Kanhere, D. G.; Blundell, S. A. Why Do Gallium Clusters Have a Higher Melting Point than the Bulk? *Phys. Rev. Lett.* **2004**, *92*, 135506.
- (41) Núñez, S.; López, J. M.; Aguado, A. Neutral and Charged Gallium Clusters: Structures, Physical Properties and Implications for the Melting Features. *Nanoscale* **2012**, *4*, 6481–6492.
- (42) Steenbergen, K.; Schebarchov, D.; Gaston, N. Electronic Effects on the Melting of Small Gallium Clusters. *J. Chem. Phys.* **2012**, *137*, 144307.
- (43) Joshi, K.; Krishnamurty, S.; Kanhere, D. “Magic Melters” Have Geometrical Origin. *Phys. Rev. Lett.* **2006**, *96*, 135703.
- (44) Chacko, S.; Kanhere, D. G.; Blundell, S. A. First Principles Calculations of Melting Temperatures For Free Na Clusters. *Phys. Rev. B* **2005**, *71*, 155407.
- (45) Lee, M. S.; Chacko, S.; Kanhere, D. G. First-Principles Investigation of Finite-Temperature Behavior in Small Sodium Clusters. *J. Chem. Phys.* **2005**, *123*, 164310.
- (46) Susan, A.; Kibey, A.; Kaware, V.; Joshi, K. Correlation Between the Variation in Observed Melting Temperatures and Structural Motifs of the Global Minima of Gallium Clusters: An *Ab Initio* Study. *J. Chem. Phys.* **2013**, *138*, 014303.
- (47) Neal, C. M.; Starace, A. K.; Jarrold, M. F. Ion Calorimetry: Using Mass Spectrometry to Measure Melting Points. *J. Am. Soc. Mass. Spectrom.* **2007**, *18*, 74–81.
- (48) Neal, C. M.; Breaux, G. A.; Cao, B.; Starace, A. K.; Jarrold, M. F. Improved Signal Stability from a Laser Vaporization Source with a Liquid Metal Target. *Rev. Sci. Instrum.* **2007**, *78*, 075108.
- (49) Jarrold, M. F.; Honea, E. C. Dissociation of Large Silicon Clusters: The Approach to Bulk Behavior. *J. Phys. Chem.* **1991**, *95*, 9181–9185.
- (50) Jarrold, M. F. Drift Tube Studies of Atomic Clusters. *J. Phys. Chem.* **1995**, *99*, 11–21.
- (51) Bohr, J. Quantum Mode Phonon Forces between Chain Molecules. *Int. J. Quantum Chem.* **2001**, *84*, 249–252.
- (52) Harrington, S.; Zhang, R.; Poole, P. H.; Sciortino, F.; Stanley, H. E. Liquid-Liquid Phase Transition: Evidence from Simulations. *Phys. Rev. Lett.* **1997**, *78*, 2409–2412.
- (53) Glosli, J. N.; Ree, F. H. Liquid-Liquid Phase Transformation in Carbon. *Phys. Rev. Lett.* **1999**, *82*, 4659–4662.
- (54) Li, Y.; Li, J.; Wang, F. Liquid–Liquid Transition in Supercooled Water Suggested by Microsecond Simulations. *Proc. Natl. Acad. Sci. U.S.A.* **2013**, *110*, 12209–12212.
- (55) Berry, R. S.; Jellinek, J.; Natanson, G. Melting of Clusters and Melting. *Phys. Rev. A* **1984**, *30*, 919–931.
- (56) Jellinek, J.; Beck, T. L.; Berry, R. S. Solid-Liquid Phase Changes in Simulated Isoenergetic  $Ar_{13}$ . *J. Chem. Phys.* **1986**, *84*, 2783–2794.
- (57) Berry, R. S. Melting and Freezing Phenomena. *Microscale Thermophys. Eng.* **1997**, *1*, 1–18.
- (58) Kunz, R. E.; Berry, R. S. Coexistence of Multiple Phases in Finite Systems. *Phys. Rev. Lett.* **1993**, *71*, 3987–3990.
- (59) Wales, D. J.; Berry, R. S. Coexistence in Finite Systems. *Phys. Rev. Lett.* **1994**, *73*, 2875–2878.
- (60) Neal, C. M.; Starace, A. K.; Jarrold, M. F. Melting Transitions in Aluminum Clusters: The Role of Partially Melted Intermediates. *Phys. Rev. B* **2007**, *76*, 054113.
- (61) Hock, C.; Bartels, C.; Straßburg, S.; Schmidt, M.; Haberland, H.; von Issendorff, B.; Aguado, A. Premelting and Postmelting in Clusters. *Phys. Rev. Lett.* **2009**, *102*, 043401.